Autofocusing Nonrigid Respiratory Motion Correction for 3D Cones Coronary MR Angiography

R Reeve Ingle[1], Holden H Wu[2], Nii Okai Addy[1], Joseph Y Cheng[1], Bob S Hu[1,3], and Dwight G Nishimura[1]

[1]*Electrical Engineering, Stanford University, Stanford, California, United States,* [2]*Department of Radiology, University of California, Los Angeles, California, United States,* [3]*Palo Alto Medical Foundation, Palo Alto, California, United States*

Target Audience MR physicists and engineers interested in image reconstruction, motion correction, cardiac imaging, or coronary angiography.

Purpose Respiratory motion of the heart is a significant challenge to coronary magnetic resonance angiography (MRA). While respiratory gating or breath-hold techniques have been used to mitigate respiratory motion artifacts, these techniques have drawbacks such as prolonging scan times or limiting spatial resolution. Retrospective correction techniques enable higher scan efficiencies but are not always capable of fully compensating the nonrigid motion of the heart. In this work, we combine a 3D cones free-breathing coronary MRA sequence [1] with a nonrigid autofocusing motion correction technique [2]. In phantom, volunteer and patient studies, we demonstrate significant improvements in the depiction of the coronary arteries using the autofocus motion correction algorithm.

Methods A free-breathing multi-phase 3D cones acquisition was used for cardiac imaging of healthy volunteers and patients at 1.5 T [1]. Sagittal and coronal 2D spiral image navigators (iNAVs) of the heart were acquired every heartbeat, before and after 3D cones data acquisition, respectively. A least-squares-based technique [1,3] was used to compute SI, AP, and RL displacements from the iNAVs using a region of interest (ROI) covering the heart. The acquired data were retrospectively corrected using an autofocusing nonrigid respiratory motion correction algorithm [2]. Multiple candidate SI, AP, and RL motion trajectories were used to reconstruct a bank of rigid-body motion-corrected 3D images. The candidate motion trajectories were obtained by scaling the measured SI, AP, and RL motion trajectories, which assumes that the motion in different regions of the heart is correlated, having the same cyclic displacement pattern due to respiratory motion. A total of 9 SI, 9 AP, and 5 RL scale factors were chosen uniformly between 0x and 2x. A gradient-entropy focusing metric [4] was used to form the final nonrigid motion-corrected image by selecting the best-focused pixels from the bank of motion-corrected images. We carried out free-breathing coronary scans on healthy volunteers and patients using ECG gating to acquire three cardiac phases (~100 ms each) during mid-diastole. Volunteer studies were acquired with an FOV of 28 x 28 x 14 cm^3 and a resolution of 1.2 x 1.2 x 1.25 mm^3 over a total of 508 heartbeats (~8.5 min), and patient studies were acquired with an FOV of 32 x 32 x 14 cm^3 and a resolution of 1.25 x 1.25 x 1.25 mm^3 over a total of 545 heartbeats (~9 min). We performed additional volunteer studies with a custom-built resolution phantom strapped around the chest. The phantom contained equally spaced vials of doped water with inner diameters of 0.75, 1.5, 2.25, 4, and 6 mm.

Results Measured motion trajectories from a volunteer study and scaled versions used by the autofocus motion correction algorithm show cyclic respiratory motion (Fig. 1). Resolution phantom images (Fig. 2) show improved sharpness with autofocus reconstruction. Reformatted maximum intensity projections (MIPs) from a free-breathing volunteer scan (Fig. 3) show significant improvements in depiction of the right coronary artery (RCA) with autofocus reconstruction. The derived SI motion map (Fig. 3d) shows the scale factors selected by the autofocus algorithm. Reformatted MIPs from a free-breathing patient scan (Fig. 4) show significant improvements in the depiction of left anterior descending (LAD) artery with autofocus motion correction.

Discussion & Conclusion Autofocus motion correction yielded significant improvements in the depiction of the coronary arteries in free-breathing coronary scans of healthy volunteers and patients. Furthermore, the algorithm was robust and never degraded image quality. Derived motion maps (e.g., Fig. 3d) agree well with intuition, showing smaller motion scales near the base of the heart and larger motion scales near the apex of the heart. Additional work will be carried out to optimize the reconstruction speed, including implementing interpolation techniques, using a subset of motion scale factors, and choosing additional motion waveforms.

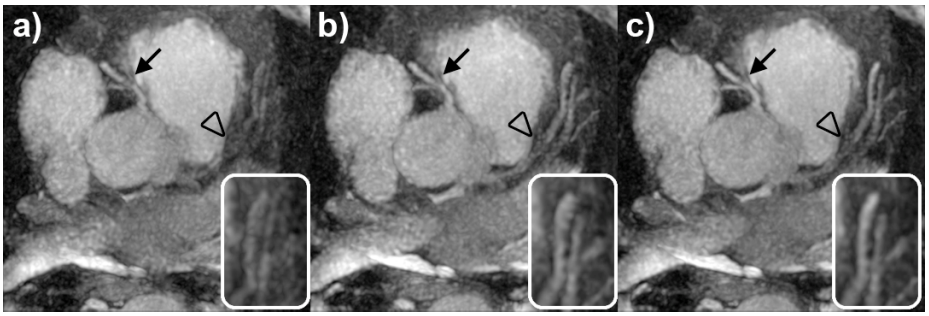

Figure 4. Reformatted MIPs from a patient study. Images are reconstructed with **(a)** no motion correction, **(b)** rigid-body motion correction, and **(c)** autofocus motion correction. Autofocus motion correction significantly improves the depiction of the LAD, especially in distal regions of the vessel (inset images). Narrowing in the RCA (arrows) and LAD (arrowheads) are well depicted in the autofocus images.

References [1] Wu HH, *et al.*, MRM early view, 2012. [2] Cheng JY, *et al.*, MRM early view, 2012. [3] Wang Y, *et al.*, MRM 36:117-123, 1996. [4] McGee KP, *et al.*, JMRI 11:174-181, 2000.

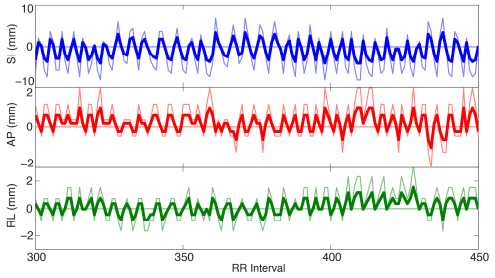

Figure 1. SI, AP, and RL motion basis set. Displacements measured from iNAVs (thick traces) were scaled (0-2x) to produce a set of candidate motion paths (0x & 2x shown as thin traces), which were used to generate a bank of motion-corrected images.

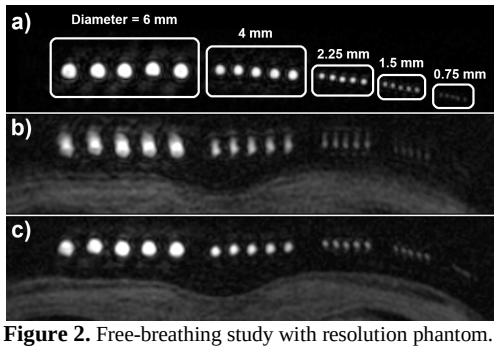

Figure 2. Free-breathing study with resolution phantom. **(a)** A static 3D cones phantom acquisition is labeled with the inner diameters of each phantom. An in-vivo acquisition with the phantoms on the chest wall is reconstructed with **(b)** no motion correction and **(c)** autofocus motion correction.

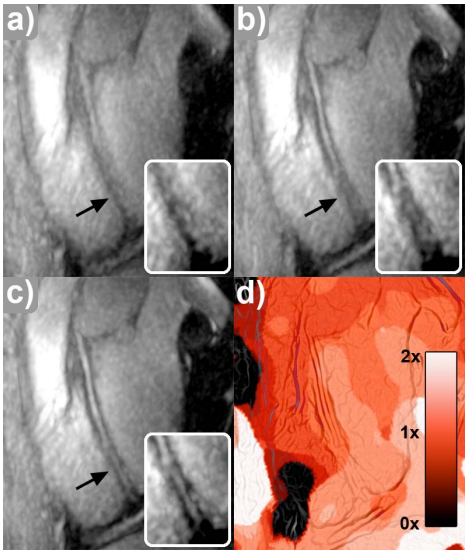

Figure 3. Reformatted thin-slab MIPs from a volunteer study. Depiction of the RCA (arrows, inset images) progressively improves in images with **(a)** no motion correction, **(b)** rigid-body correction, and **(c)** autofocus motion correction. The derived SI motion map **(d)** shows the SI scale factors selected by the autofocus algorithm.